

Article

Absolute Configurations and Chitinase Inhibitions of Quinazoline-Containing Diketopiperazines from the Marine-Derived Fungus *Penicillium polonicum*

Xing-Chen Guo ^{1,†}, Ya-Hui Zhang ^{1,†}, Wen-Bin Gao ², Li Pan ³, Hua-Jie Zhu ^{1,*} and Fei Cao ^{1,*} 

¹ College of Pharmaceutical Sciences, Institute of Life Science and Green Development, Key Laboratory of Medicinal Chemistry and Molecular Diagnosis of Ministry of Education, Hebei University, Baoding 071002, China; guoxingchen92@163.com (X.-C.G.); 15689932652@163.com (Y.-H.Z.)

² College of Life Science, Cangzhou Normal University, Cangzhou 061001, China; wenbinxing@yeah.net

³ State Key Laboratory of NBC Protection for Civilian, Beijing 102205, China; bk6180b@163.com

* Correspondence: hjzhu2019@163.com (H.-J.Z.); caofei542927001@163.com (F.C.)

† These authors contributed equally to this work.

Received: 12 August 2020; Accepted: 16 September 2020; Published: 21 September 2020



Abstract: Three new quinazoline-containing diketopiperazines, polonimides A–C (1–3), along with four analogues (4–7), were obtained from the marine-derived fungus *Penicillium polonicum*. Among them, 2 and 4, 3 and 5 were epimers, respectively, resulting the difficulty in the determination of their configurations. The configurations of 1–3 were determined by 1D nuclear overhauser effect (NOE), Marfey and electron circular dichroism (ECD) methods. Nuclear magnetic resonance (NMR) calculation with the combination of DP4plus probability method was used to distinguish the absolute configurations of C-3 in 3 and 5. All of 1–7 were tested for their chitinase inhibitory activity against *OfHex1* and *OfChi-h* and cytotoxicity against A549, HGC-27 and UMUC-3 cell lines. Compounds 1–7 exhibited weak activity towards *OfHex1* and strong activity towards *OfChi-h* at a concentration of 10.0 μ M, with the inhibition rates of 0.7%–10.3% and 79.1%–95.4%, respectively. Interestingly, 1–7 showed low cytotoxicity against A549, HGC-27 and UMUC-3 cell lines, suggesting that good prospect of this cluster of metabolites for drug discovery.

Keywords: marine-derived fungus; *Penicillium polonicum*; quinazoline; diketopiperazine; bioactivity

1. Introduction

The biosynthetic gene clusters in one fungus species usually destine the generation of structurally versatile secondary metabolites [1]. In recent years, plenty of structurally-unique secondary metabolites have been obtained from the marine-derived fungi [2,3]. However, natural compounds from fungi usually have a high degree of chiral variety, forming one structure with different configurations, which caused a challenging task of determination for their configurations, especially when the molecules displayed high conformational flexibility [3]. Meanwhile, the stereochemistry of molecules has become one of the most important features of chiral natural products, which play a fundamental role in biology, chemistry and medicine. Thus, assigning the stereochemical characterizations attracted more and more attentions in the field of natural medicinal chemistry [4,5]. In our research on structurally-unique and biologically-active metabolites from the marine-derived fungi, the fungal strain *Penicillium polonicum* HBU-114, whose EtOAc extract exhibited the original thin-layer chromatography (TLC) and high performance liquid chromatography-under voltage (HPLC-UV) profiles of the secondary metabolites, differed from the other fungi, attracted our attention. HPLC-guided separation resulted in the isolation of three new quinazoline alkaloids, polonimides A–C (1–3) and four known analogues, aurantiomide

C (4) [6], anacine (5) [6], aurantiomide A (6) (Figure S24) [6] and aurantiomide B (7) (Figure S25) [6] (Figure 1). Herein, we report the isolation, absolute configurations and bioactivity of these compounds.

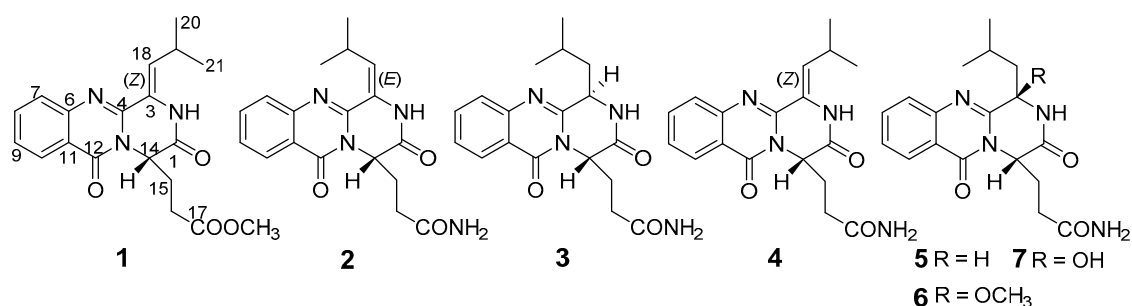


Figure 1. Chemical structures of 1–7.

2. Results

Polonimide A (1) was obtained as a yellow amorphous powder. The molecular formula of $C_{19}H_{21}N_3O_4$ (11 degrees of unsaturation) was established by the positive high resolution electrospray ionization mass spectroscopy (HRESIMS) data. The downfield of 1H NMR spectrum (Table 1, Figure S1) for 1 exhibited six proton signals, including one nitrogen-hydrogen proton signal δ_H 10.49 and five olefin proton signals (δ_H 8.13, 7.84, 7.69, 7.52 and 6.22). In addition, the 1H NMR spectrum of 1 showed one methoxy singlet δ_H 3.42 and two methyl doublets (δ_H 1.08 and 1.05). The ^{13}C NMR spectrum (Table 2, Figure S2) of 1 revealed three carbonyl carbon signals (δ_C 159.9, 165.2 and 171.8). With careful inspection and analyses of the 1D-NMR and HSQC data (Figure S3), it was found that 1 shares the same quinazolinone core as aurantiomide C (4), a diketopiperazine alkaloid isolated from the fungus *Penicillium aurantiogriseum* [6]. The main differences between 1 and 4 were the presence of an additional methoxy group (δ_H 3.42; δ_C 51.3) and the absence of two nitrogen-hydrogen proton signals (δ_H 7.27 and 6.73 in 4) (Figure S22) in 1, suggesting the presence of 17-OCH₃ group in 1 instead of 17-NH₂ group in 4. The above deduction was further confirmed by the key HMBC correlation from -OCH₃ to C-17 of 1 (Figure 2, Figure S5).

Table 1. 1H NMR Data (δ) of 1–3 and 5 (600 MHz, DMSO- d_6 , J in Hz).

No.	1	2	3	5
2	10.49, brs	10.49, brs	8.53, brs	8.91, d (4.2)
3	-	-	4.74, dd (7.8, 3.6)	4.40–4.43, m
7	7.69, d (7.8)	7.65, d (8.4)	7.68, d (8.4)	7.66, d (7.8)
8	7.84, dd (7.8, 7.2)	7.86, dd (8.4, 7.2)	7.85, dd (8.4, 7.2)	7.84, dd (7.8, 7.2)
9	7.52, dd (7.8, 7.2)	7.57, dd (7.8, 7.2)	7.56, dd (7.8, 7.2)	7.54, dd (7.8, 7.2)
10	8.13, d (7.8)	8.16, d (7.8)	8.15, d (7.8)	8.15, d (7.8)
14	5.19, dd (6.6, 6.0)	5.12, dd (6.6, 6.0)	5.09, dd (7.8, 6.6)	4.86, dd (9.0, 6.0)
15	2.12–2.17, m	2.02–2.06, m	2.17–2.20, m	2.09–2.14, m
-	2.02–2.07, m	-	2.12–2.14, m	2.01–2.06, m
16	2.38–2.43, m	2.11–2.14, m	2.21–2.26, m	2.30–2.35, m
-	2.32–2.37, m	-	-	2.38–2.44, m
18	6.22, d (10.8)	5.54, d (9.6)	2.28–2.31, m	1.74–1.81, m
-	-	-	1.64–1.68, m	-
19	2.94–3.00, m	3.74–3.79, m	2.07–2.11, m	1.87–1.93, m
20	1.05, d (6.6)	1.02, d (6.6)	0.97, d (6.6)	0.97, d (6.6)
21	1.08, d (6.6)	1.20, d (6.6)	0.98, d (6.6)	0.99, d (6.6)
17-OCH ₃	3.42, s, 3H	-	-	-
17-NH ₂	-	7.26, s	7.29, s	7.36, s
-	-	6.71, s	6.75, s	6.78, s

Table 2. ^{13}C NMR Data (δ) of 1–3 and 5 (150 MHz, DMSO- d_6).

No.	1	2	3	5
1	165.2, C	165.5, C	167.9, C	166.6, C
3	126.6, C	124.8, C	55.7, CH	54.9, CH
4	145.5, C	144.8, C	152.2, C	152.0, C
6	147.0, C	146.7, C	146.6, C	147.0, C
7	126.3, CH	127.5, CH	127.3, CH	126.7, CH
8	134.7, CH	134.7, CH	134.7, CH	134.7, CH
9	126.7, CH	127.2, CH	127.0, CH	126.7, CH
10	125.3, CH	126.3, CH	126.3, CH	126.2, CH
11	119.7, C	119.7, C	119.8, C	119.7, C
12	159.9, C	159.7, C	160.1, C	160.1, C
14	54.3, CH	54.7, CH	50.7, CH	53.8, CH
15	27.2, CH ₂	28.0, CH ₂	25.6, CH ₂	29.4, CH ₂
16	29.2, CH ₂	30.9, CH ₂	31.3, CH ₂	32.2, CH ₂
17	171.8, C	172.4, C	172.7, C	172.8, C
18	127.1, CH	131.0, CH	39.0 ^a , CH ₂	47.2, CH ₂
19	25.0, CH	26.5, CH	23.8, CH	24.0, CH
20	22.0, CH ₃	23.1, CH ₃	23.3, CH ₃	23.0, CH ₃
21	22.3, CH ₃	22.4, CH ₃	21.7, CH ₃	21.4, CH ₃
17-OCH ₃	51.3, CH ₃	-	-	-

^a which was speculated in the HSQC spectrum according to the correlations from δ_{H} 2.29/1.66 to δ_{C} 39.0.

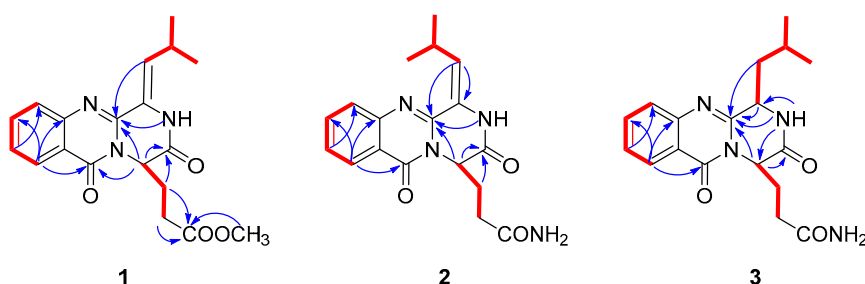


Figure 2. ^1H - ^1H correlation spectroscopy (COSY) (Figure S4) (bold) and Key heteronuclear multiple bond correlation (HMBC) (arrows) of 1–3.

Polonimide B (**2**) was also obtained as a yellow amorphous powder with the molecular formula $\text{C}_{18}\text{H}_{20}\text{N}_4\text{O}_3$ (11 degrees of unsaturation) by HRESIMS spectrum. Detailed analysis of the 1D and 2D NMR spectra of **2** (Figures S7–S11), it was found that **2** was an analogue of **1**. Combination with their NMR (Tables 1 and 2) and HRESIMS data (Figures S6 and S13), showed that **2** differed from **1** by loss of an OCH_3 unit (δ_{H} 3.42, δ_{C} 51.3 in **1**) and replaced by a NH_2 unit (δ_{H} 7.26 and 6.71 in **2**) in **2**. Combined analysis of the differences existed in the chemical shifts of H-18, H-19, C-18 and C-19 between **2** and **4** indicated that **2** was an isomer of **4** with different geometries of the double bond $\text{C}_3=\text{C}_{18}$.

Polonimide C (**3**) was obtained with the molecular formula of $\text{C}_{18}\text{H}_{22}\text{N}_4\text{O}_3$ (10 degrees of unsaturation) by the positive HRESIMS data (Figure S21). Analysis of the ^1H and ^{13}C NMR spectra of **3** (Tables 1 and 2, Figures S14–S17), revealed **3** had the same anacine core structure as **2**. The main differences between **3** and **2** were the NMR chemical shifts of 2-NH, C-4, C-19 and the presence of one nitrogen-bearing methine (δ_{H} 4.74, δ_{C} 55.7 in **3**), one methylene (δ_{H} 2.29/1.66, δ_{C} 39.0 in **3**) and the absence of one olefinic quaternary carbon (C-3 in **2**) and methylene (C-18 in **2**) in **3**. It was inferred that the double bond between C-3 and C-18 in **2** was reduced in **3**, which could also be verified by the ^1H - ^1H COSY correlations from H-3 (δ_{H} 4.74) to H-18 (δ_{H} 2.29, δ_{H} 1.66) and from H-18 to H-19 (δ_{H} 2.09) of **3** (Figure S18). The chemical structure of **3** was further confirmed by the key HMBC correlations from NH-2 to C-3, C-4 and C-14, from H-14 to C-1 and C-4, from H-18 to C-4 and from H-3 to C-4 of **3** (Figure 2, Figure S19). It should be noted that the chemical structure of **3** could be found in the

Scifinder database with the cas registry number 154725-83-4. However, the chemical structure of cas 154725-83-4 was the same as anacine (5), which was originally proposed as a benzodiazepine structure by Mantle and co-workers [7] but was revised as a quinazoline structure by Sim and co-workers [8].

The geometries of the double bond $C_3=C_{18}$ in **1** and **2** were established with their selective 1D nuclear overhauser effect (NOE) experiments (Figure S12). In compound **1**, the irradiation of 2-NH (δ_H 10.49) resulting in no obvious enhancement of H-18 (δ_H 6.22) indicated that 2-NH and H-18 might be *trans* oriented; the downfield chemical shift of H-18 caused by the deshielding effect of 4-imine also confirmed the *Z* geometries of the double bond $C_3=C_{18}$. Whereas, in compound **2**, irradiation of 2-NH (δ_H 10.49) resulted in enhancement of H-18 (δ_H 5.54), was ascertained that H-18 and 2-NH in **2** were *cis* oriented, which indicated the geometries of the double bond $C_3=C_{18}$ was *E*.

In compound **3**, the chemical shift at C-14/15/18 (δ_C 50.7/25.6/39.0) showed some deviation from that of **5** (C-14/15/18, δ_C 53.8/29.4/47.2) (Figure S23), which suspected **3** and **5** were a pair of epimers. The position of H-3 and H-18 was in 1,4 relation, which meant it was too far to provide the (nuclear overhauser effect spectroscopy) NOESY correlations for **3** (Figure S20), thus the relative configuration between C-3 and C-14 in **3** could not be determined.

The absolute configuration of the Glutamine residue at C-14 position of **1–3** was established by the combination of Marfey's method and comparing the computed electronic circular dichroism (ECD) spectra with their experimental results. The HPLC analysis showed that the Glutamine residue in compounds **1–3** was L-Glutamine (Figure 3). Simultaneously, the ECD curve displayed that the predicted ECD spectra of **14S-1/2/3** look similar to the experimental results of **1–3** (Figure 4, Figures S26–S31). Therefore, the absolute configuration of C-14 was assigned as *S* in **1–3**.

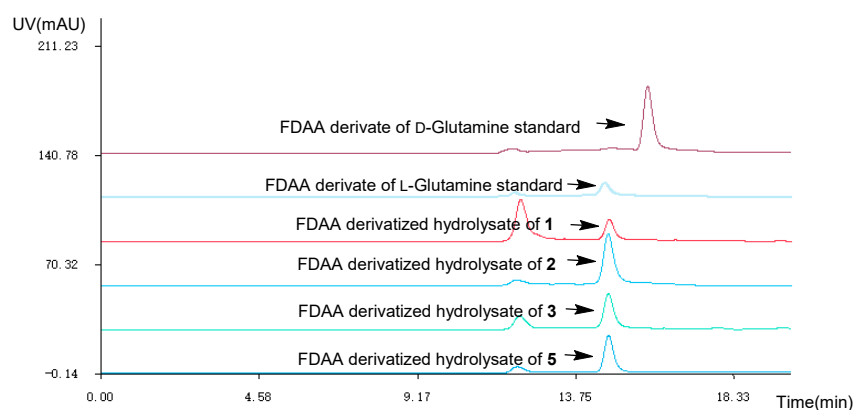


Figure 3. HPLC at 254 nm of the Marfey's analysis (1-fluoro-2-4-dinitrophenyl-5-L-alanine amide (FDAA) derivate of L-Glutamine standard t_R 14.5 min; FDAA derivate of D-Glutamine standard t_R 15.8 min; MeOH-H₂O (70:30, *v:v*), *v* = 2.0 mL/min).

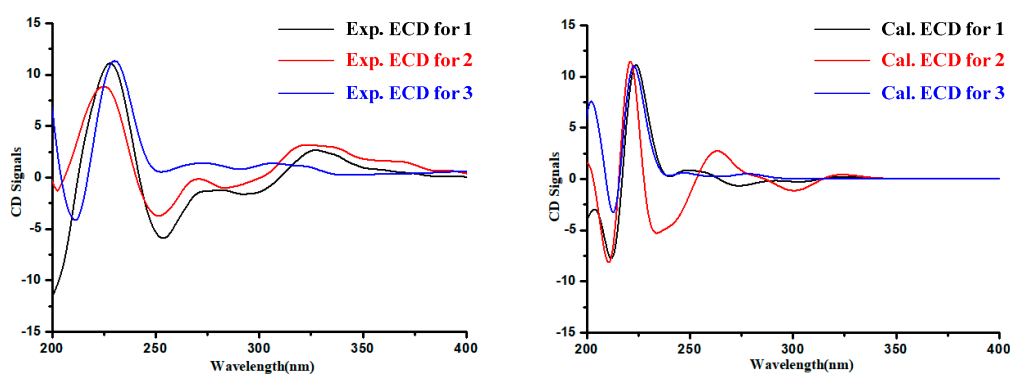


Figure 4. Experimental and calculated electronic circular dichroism (ECD) spectra of **1–3**.

Analysis of the structure of **3** and the experimental ECD curves of **1–3** (Figure 4) revealed the absolute configuration of C-3 in **3** contributed little to its ECD Cotton effects. Since the absolute configuration at C-14 has been determined by Marfey's analysis, the ^{13}C NMR chemical shift calculation was applied to confirm the C-3 absolute configuration of **3**, with the combination of DP4plus probability method, which is one of the most sophisticated and popular strategies for chemical structure interpretation [9]. Both **3** and **5** were performed with two configurations [(3*R*,14*S*)-**3/5** and (3*S*,14*S*)-**3/5**] for NMR calculations. The calculated NMR data of **3** and **5** were all together compared with the experimental results, respectively. The result showed that (3*R*,14*S*)-**3** was more likely than (3*S*,14*S*)-**3** (100% vs. 0%) compared with the experimental data of **3** and (3*S*,14*S*)-**5** is more likely than (3*R*,14*S*)-**5** (100% vs. 0%) compared with the experimental data of **5** (Figures S32 and S33). Subsequently, the absolute configurations of **3** and **5** were assigned as 3*R*,14*S*-**3** and 3*S*,14*S*-**5**, respectively.

The insect enzymes GH20 β -*N*-acetyl-D-hexosaminidase *OfHex1* and GH18 chitinase *OfChi-h* represent important chitinolytic enzymes found in the agricultural pest *Ostrinia furnacalis* (Guenée) and inhibition of these enzymes have been considered a promising strategy for the development of eco-friendly pesticides. All of the isolated compounds were evaluated for their *in vitro* inhibitory potency against *OfHex1* and *OfChi-h*, by using MU-GlcNAc and MU-(GlcNAc)₂ as substrates, respectively. Compounds **1–7** exhibited weak activities towards *OfHex1* and strong activities towards *OfChi-h* at a concentration of 10.0 μM (Table 3), suggesting some valuable clues regarding the structure-activity relationships. Compound **1** bearing the methoxy group on C-17 could weaken the inhibitory activities against *OfHex1* and *OfChi-h* compared to **4**. Moreover, in compounds **2** and **4**, the double bond of *Z* configuration of **4** showed better activities, indicated that the geometries of the double bond C₃=C₁₈ in **2** and **4** had a direct influence on the inhibitory efficiency against *OfHex1* and *OfChi-h*.

Table 3. Chitinase Inhibitory Activity for Compounds **1–7**.

Compounds	Inhibition Rate (%)			
	<i>OfHex1</i>		<i>OfChi-h</i>	
	10.0 μM	10.0 μM	1.0 μM	0.2 μM
1	0.7	91.9	75.1	28.1
2	3.8	79.1	74.3	4.0
3	1.4	86.1	73.1	15.8
4	10.3	95.4	85.5	23.2
5	6.8	92.3	75.9	20.1
6	7.4	90.5	83.9	3.2
7	5.9	85.7	77.6	21.7

To further explore the inhibition mechanism of these quinazoline-containing diketopiperazines towards *OfHex1* and *OfChi-h*, compounds **1** and **4** were firstly selected for investigating the binding mode using molecular docking to *OfChi-h* (Figure 5a) and *OfHex1* (Figure 5c), respectively.

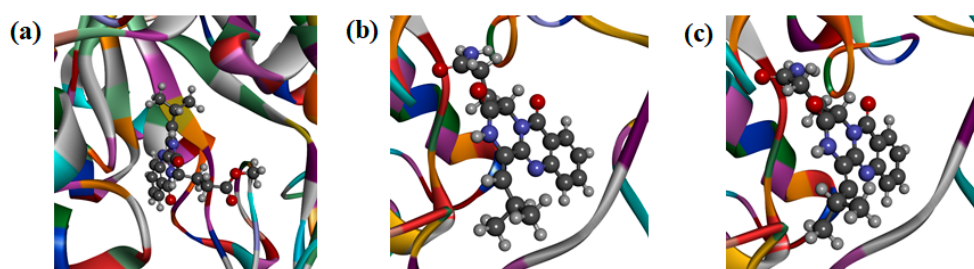


Figure 5. (a) Docking simulations of **1** with target protein *OfChi-h*. (b) Docking simulations of **2** with target protein *OfHex1*. (c) Docking simulations of **4** with target protein *OfHex1*.

Compound **1** was found to tightly bind to the entire active pocket of *OfChi-h* (Figure S34). Three hydrogen bonds, with bond lengths of 2.67 Å, 2.82 Å and 2.91 Å, were formed by the C-12 cycloamide-carbonyl group and C-17 ester carbonyl group of **1** with the guanidine group of ARG439 (Figure S35). The benzene ring and the lactam ring of **1** had a π -sulfur interaction with the sulfur atom of methionine MET381, with the operating distances of 4.57 Å and 5.01 Å, respectively (Figure S36). It was also found that **1** had a π - π stacking with the benzene rings of Trp268 and Phe309 (Figure S37). Alkyl hydrophobic interactions were showed between the C-18 isopropyl of **1** and Ala355/Met381 and between the 17-OCH₃ of **1** and Val469 (Figure S38). In addition, the C-18 isopropyl of **1** bound to Tyr156 and Phe184 through mixed π /alkyl hydrophobic interactions (Figure S39).

Compound **4** was found to bind to the *OfHex1* in a “U” conformation (Figure S40). The C-17 carbonyl and 17-NH₂ of **4** formed hydrogen bonds on the guanidine group of ARG220 and the carboxyl of ASP367, respectively (Figure S41). Compound **4** had a π -anion with the carboxyhydroxyl oxygen anion in the residue of GLU368 (Figure S42) and π - π stacking interaction with the indole ring of Trp490 (Figure S43). It was also found that the C-18 isopropyl group of **4** had an alkyl hydrophobic interaction with the isopropyl group of Val484 (Figure S44). Mixed π /alkyl hydrophobic interactions were also found between the C-18 isopropyl group of **4** and Trp322/Trp483 and between the benzene and lactam rings of **4** and the isopropyl group of Val327 (Figure S45).

It is noteworthy that the geometric isomers **2** and **4** had different activity value, urging to investigate the binding mode of **2** and *OfHex1* (Figure 5b). From the FlexibleDocking results, it was found that the π -anion between **4** and the carboxyhydroxyl oxygen anion in GLU368 was absent in **2**. Moreover, the amocarbonyl group of **4** and guanidine group of Arg220 formed two hydrogen bond interactions, while there was only one N-H hydrogen bond interaction between **2** and Arg220 (Figure S46). The above results could explain **2** was less active than **4**.

All of the isolated compounds (**1**–**7**) were also evaluated for their cytotoxic activities against human lung cancer cell line (A549), human gastric cancer cell line (HGC-27), human bladder cancer cell line (UMUC-3) and a non-tumoral cell line, human gastric epithelium (GES-1) (Table S1). Among them, only compound **5** exhibited cytotoxicities against the three cell lines (IC₅₀ = 6.0, 6.2, 7.2 μ M, respectively).

3. Discussion

Diketopiperazines, which have been found to occur from a wide range of fungi, display a variety of bioactivities from antineoplastic, antifungal, antibacterial, to anti-inflammatory effects and have the potential to be used in the development of new drugs [10,11]. Among them, quinazoline-containing diketopiperazines, generally possess a tricyclic core of benzene–pyrimidinone–diketopiperazine, are relatively rare. Due to the configurational flexibility of the residue and little contribution to ECD Cotton effects, it was hard to assign the absolute configurations of C-3 of **3** and **5**. In the course of our study, the ¹³C NMR chemical shift calculation with the combination of DP4plus probability method was applied to assign and distinguish the C-3 absolute configuration of **3** and **5**. Furthermore, the isomers **2** and **4** and **3** and **5** showed different activity value, suggesting that the geometries of the double bond C₃=C₁₈ in **2** and **4** and the configuration at C-3 in **3** and **5**, may play an important role for bioactivities.

4. Experimental Section

4.1. General Experimental Procedures

Optical rotatory (OR) and ECD data were performed on a JASCO P-1020 and JASCO J-815 spectrometers (JASCO Corporation, Tokyo, Japan), respectively. UV and IR spectra were gathered using a Perkin-Elmer model 241 spectrophotometer (Perkin-Elmer Corporation, MA, USA) and a Nicolet NEXUS 470 spectrophotometer (Thermo Corporation, MA, USA), respectively. 1D/2D NMR spectra were measured on a Bruker AV-600 spectrometer (Thermo Corporation, Karlsruhe, Germany). HRESIMS data were recorded on a Thermo Scientific LTQ Orbitrap XL spectrometer (Thermo Corporation, MA, USA). Semipreparation HPLC (Shimadzu LC-20AT system) (Hitachi High

Technologies, Tokyo, Japan) was operated using a SPD-M20A detector (Hitachi High Technologies, Tokyo, Japan) and a Waters RP-18 column (Waters Corporation, Manchester, UK). The material of Sephadex LH-20 and Silica gel used for chromatographic separation were the same as those in our previous literature [4].

4.2. Isolation of the Fungal Material

The fungal strain HBU-114 with the National Center for Biotechnology Information (NCBI) GenBank accession number MN623481, collected from the Bohai Sea (Huanghua, Hebei Province, China, June 2016), was identified as *Penicillium polonicum* by the molecular biological method of amplification and sequencing of the DNA sequences of the ITS region of the rRNA gene. It was deposited in the College of Pharmaceutical Sciences, Hebei University. The fungus HBU-114 was cultivated in rice medium (80 g rice, 60 mL H₂O, 2.0 g sea salt in each Erlenmeyer flask) in a total of forty Erlenmeyer flasks at 28 °C for 28 days. Mixture of CH₂Cl₂/MeOH (1:1, v:v) was used to extract the fermented rice substrate for six times. The organic extract was evaporated to remove solvent, after which it was extracted with EtOAc and H₂O (1:1, v:v) for six times and evaporated to dryness to give the EtOAc extract (10.8 g). The extract was separated by silica gel column chromatography (CC) with EtOAc-petroleum ether (PE) (0–100% EtOAc) to give six fractions (Fr.1–Fr.6). Fr.5, eluted with 80% EtOAc–PE (4:1, v:v), was applied to a Sephadex LH-20 CC (CH₂Cl₂/MeOH (1:1, v:v)) to remove the pigment to give Fr.5-1–Fr.5-2. Then, Fr.5-2 was further separated by silica gel CC using mixtures of CH₂Cl₂ and MeOH (20:1, v:v) to offer Fr.5-2-1–Fr.5-2-4. Among them, Fr.5-2-2 was purified by ODS column eluted with 80% MeOH/H₂O and then separated by HPLC on a waters RP-18 column (XBridge OBD, 5 μm, 10 × 250 mm, MeOH-H₂O (40:60, v:v) to obtain polonimide A (**1**) (6.5 mg, 51.0 min), polonimide B (**2**) (5.6 mg, 36.0 min) and **7** (8.9 mg, 24.5 min), respectively. Fr.5-2-3 was chromatographed on silica gel eluting with CH₂Cl₂–MeOH (30:1) and further purified by HPLC on a waters RP-18 column (XBridge OBD, 5 μm, 10 × 250 mm, MeOH-H₂O (40:60, v:v) to give polonimide C (**3**) (8.5 mg, 33.0 min), **4** (355.2 mg, 21.0 min), **5** (3.4 mg, 17.5 min) and **6** (8.2 mg, 37.5 min), respectively.

Polonimide A (1): amorphous powder; $[\alpha]_D^{20} +14.0$ (c 0.3, CH₃OH); UV (MeOH) λ_{\max} (log ϵ) 245 (1.50) nm; ECD (MeOH) λ_{\max} ($\Delta\epsilon$) 222 (+3.4), 245 (+1.1) nm; IR (KBr) ν_{\max} 3198, 1636, 1602, 1588, 1563, 761 cm⁻¹; ¹H and ¹³C NMR, see Tables 1 and 2; HRESIMS m/z 378.1424 [M + Na]⁺ (calcd for C₁₉H₂₁N₃O₄Na, 378.1424 [M + Na]⁺).

Polonimide B (2): amorphous powder; $[\alpha]_D^{20} +24.0$ (c 0.3, CH₃OH); UV (MeOH) λ_{\max} (log ϵ) 350 (1.50) nm; ECD (MeOH) λ_{\max} ($\Delta\epsilon$) 222 (+3.4), 315 (+1.0) nm; IR (KBr) ν_{\max} 3191, 1634, 1601, 1579, 1566, 765 cm⁻¹; ¹H and ¹³C NMR, see Tables 1 and 2; HRESIMS m/z 378.1408 [M + Na]⁺ (calcd for C₁₈H₂₀N₄O₃Na, 378.1433 [M + Na]⁺).

Polonimide C (3): amorphous powder; $[\alpha]_D^{20} +171.0$ (c 0.3, CH₃OH); UV (MeOH) λ_{\max} (log ϵ) 330 (1.50) nm; ECD (MeOH) λ_{\max} ($\Delta\epsilon$) 210 (-0.7), 228 (1.7) nm; (KBr) ν_{\max} 3193, 1633, 1603, 773 cm⁻¹; ¹H and ¹³C NMR, see Tables 1 and 2; HRESIMS m/z 365.1568 [M + Na]⁺ (calculated for C₁₈H₂₂N₄O₃Na, 365.1590 [M + Na]⁺).

4.3. General Computational Procedure

Quantum chemical calculations for **1–3** and **5** were carried out on the basis of previous references (gas phase) [12–14]. Chemical structures of **1–3** and **5** were constructed and used for conformational searches using MMFF94S force field by the BARISTA 7.0 software (CONFLEX Corporation Tokyo, Japan). Of all the geometries, those with relative energy of 0–10.0 kcal/mol (93 stable conformers for **1**, 85 stable conformers for **2**, 49 stable conformers for **3** and 58 stable conformers for **5**) were optimized at the B3LYP/6-311+G(d) level, then those with a relative energy of 0–2.5 kcal/mol (15 conformers for **1**, 27 conformers for **2**, 9 conformers for **3** and 16 conformers for **5**) were chosen for ECD calculations at the B3LYP/6-311++G(2d,p) level and simulated using SpecDis 1.71 [15]. In addition, DP4plus applications were used to assign the absolute configurations of **3** and **5**, the optimized conformers were calculated

at the B3LYP/6-311+G(d,p)//B3LYP/6-311+G(d,p) level for the unshielded tensor values. All of the calculations were processed with Gaussian 09 package [16].

4.4. Preparation and Analysis of Marfey's Derivatives

Compounds 1–3 (0.2 mg, respectively), dissolved in 0.5 mL of 6N HCl under the temperature of 110 °C, were hydrolyzed for 4 h. After temperature of the solutions dropped to 25 °C, the mixture were evaporated to dryness under vacuum with addition of distilled H₂O to remove the trace HCl, then redissolved it in H₂O (50 µL). The divided hydrolysate were treated with 200 µL of 0.5% (w/v) 1-fluoro-2-4-dinitrophenyl-5-L-alanine amide (FDAA) in acetone and 20 µL 1N NaHCO₃ in order of precedence. The mixture was stirred at 45 °C for 40 min and then it was quenched through the addition of 20 µL of 2N HCl. The mixture was evaporated to give the resulting residues, which was dissolved in MeOH (20 µL) [17]. Similarly, the standard amino acid L-Glutamine and D-Glutamine were derivatized with FDAA using the same procedure as that of 1–3. And the derivatives were analyzed by HPLC with linear isocratic elution (MeOH-H₂O (70:30, v:v)) detected at 254 nm.

4.5. Enzymes Inhibitory Activity Assay

In a final assay volume of 100 µL, enzyme was incubated with substrate (20 µM MU-(GlcNAc)₂ for *OfChi-h* and 50µM MU-GlcNAc for *OfHex1*) in 20 mM sodium phosphate buffer (pH 6.0 for *OfChi-h*, pH 6.5 for *OfHex1*) containing 10 µM inhibitor at 30 °C. The reaction in the absence of inhibitor was used as a control. After reacting for an appropriate time (30min), an equal volume of 0.5 M Na₂CO₃ was added to the reaction mixture to terminate the reaction and the fluorescence of the liberated MU was quantitated using a Varioskan Flash microplate reader, with excitation and emission wavelengths of 360 and 450 nm [18].

4.6. Molecular Docking

The complex crystal structure of *OfHex1*-PUGNAc (Protein Data Bank (PDB) entry code: 3OZP) [19] or *OfChi-h*-chitohepatose (PDB entry code: 5GQB) [20] was used as the starting model for molecular docking employing the Discovery Studio 2017 software. Before docking calculations, conformational searches of the compounds 1 and 4 were performed with the GMMX conformer calculation (Force field: MMFF94, energy window: 5.0 kcal/mol) in GaussView 6.0. Then, the top 5 conformations with the lowest energy were optimized at the B3LYP/6-31G(d) basis set using density functional theory (DFT) in Gaussian 16. To simulate real conditions, the solvent effects of H₂O were studied using the solvation model based on density (SMD). For the protein, the protein preparation processes were undergone, such as removing water molecules, adding hydrogen atoms and supplementing amino acid residues. The Flexible Docking protocol, which allows for some receptor flexibility during docking of flexible ligands [21] that employs CHARMM in Discovery Studio 2017 software, was used in this study. The receptor binding sites were determined from the PDB site records.

4.7. Cytotoxic Assay

All of the isolated compounds 1–7 were evaluated for cytotoxic activity in vitro according to MTT method [22]. Three human tumor cell lines were included—human lung cancer cell line (A549), human gastric cancer cell line (HGC-27), human bladder cancer cell line (UMUC-3) and a non-tumoral cell line, human gastric epithelium (GES-1). The positive control was cisplatinium (DDP).

Cell lines and cell culture Human A549 and HGC-27 cancer cells were obtained from Chinese Academy of Medical Sciences, Basic Medicine Cell Center (Beijing, China). Human UMUC-3 cancer cells were obtained from Cell Resource Center, Shanghai Institute of Life Sciences, Chinese Academy of Sciences (Shanghai, China). Cells were cultured in RPMI-1640 media supplemented with 10% fetal bovine serum (FBS), 100 U/mL penicillin, and 100 mg/mL streptomycin at 37 °C in a 5% CO₂ atmosphere.

5. Conclusions

Three new quinazoline alkaloids polonimides A–C (**1–3**), were obtained from the marine-derived fungus *Penicillium polonicum*. The relative and absolute configurations of **1–3** were comprehensively determined by combination of 1D NOE experiments, modified Marfey's analysis, ECD and NMR chemical shift calculations. The quinazoline-containing diketopiperazines (**1–7**) with low cytotoxicity but potent chitinase inhibitory activity also indicated good prospect of this cluster of metabolites for drug discovery.

Supplementary Materials: The following are available online at <http://www.mdpi.com/1660-3397/18/9/479/s1>, Figures S1–S25: 1D and 2D NMR and HRESIMS spectra of the **1–3**, Figures S26–S31: Experimental and calculated ECD spectra of **1–5**, Figures S32 and S33: The data of DP4plus method of **3** and **5**, Figures S34–S46: molecular docking of **1, 2, 4**, Table S1: Comparison of the data of DP4plus method of compound **3** and **5**, Table S2: Cytotoxic activity data of compounds **1–7**, Tables S3–S9: The coordinate for the conformer of **1–5** for calculations.

Author Contributions: X.-C.G. and Y.-H.Z. contributed to the fermentation, extraction and isolation; W.-B.G. contributed to the bioactivities test; L.P. contributed to the molecular docking; F.C. and H.-J.Z. was the project leader, organizing and guiding the experiments and manuscript writing. All authors have read and agreed to the published version of the manuscript.

Funding: This work was supported by the National Natural Science Foundation of China (Nos. 41606174; 21877025), the Scientific research Foundation of Hebei educational committee (No. BJ2020048), the Natural Science Interdisciplinary Research Program of Hebei University (No. DXK201913) and the High Performance Computer Center of Hebei University.

Conflicts of Interest: The authors declare no conflict of interest.

References

1. Xu, W.; Dhingra, S.; Chooi, Y.H.; Calvo, A.M.; Lin, H.C.; Tang, Y. The fumagillin biosynthetic gene cluster in *Aspergillus fumigatus* encodes a cryptic terpene cyclase involved in the formation of β -trans-bergamotene. *J. Am. Chem. Soc.* **2013**, *135*, 4616–4619.
2. Carroll, A.R.; Copp, B.R.; Davis, R.A.; Keyzers, R.A.; Prinsep, M.R. Marine natural products. *Nat. Prod. Rep.* **2019**, *36*, 122–173. [[CrossRef](#)] [[PubMed](#)]
3. Hou, X.M.; Liang, T.M.; Guo, Z.Y.; Wang, C.Y.; Shao, C.L. Discovery, absolute assignments, and total synthesis of asperversiamides A–C and their potent activity against *Mycobacterium marinum*. *Chem. Commun.* **2019**, *55*, 1104–1107. [[CrossRef](#)] [[PubMed](#)]
4. Zhu, A.; Yang, M.Y.; Zhang, Y.H.; Shao, C.L.; Wang, C.Y.; Hu, L.D.; Cao, F.; Zhu, H.J. Absolute configurations of 14,15-hydroxylated prenylxanthenes from a marine-derived *Aspergillus* sp. fungus by chiroptical methods. *Sci. Rep.* **2018**, *8*, 10621–10630. [[CrossRef](#)] [[PubMed](#)]
5. Cao, F.; Shao, C.L.; Liu, Y.F.; Zhu, H.J.; Wang, C.Y. Cytotoxic serrulatane-type diterpenoids from the gorgonian euplexaura sp. and their absolute configurations by vibrational circular dichroism. *Sci. Rep.* **2017**, *7*, 12548–12555. [[CrossRef](#)] [[PubMed](#)]
6. Xin, Z.H.; Fang, Y.C.; Du, L.; Zhu, T.J.; Duan, L.; Chen, J.; Gu, Q.Q.; Zhu, W.M. Aurantiomides A–C, quinazoline alkaloids from the sponge-derived fungus *Penicillium aurantiogriseum* SP0-19. *J. Nat. Prod.* **2007**, *70*, 853–855. [[CrossRef](#)] [[PubMed](#)]
7. Boyes-Korkis, J.M.; Gurney, K.A.; Penn, J.; Mantle, P.G.; Bilton, J.N.; Sheppard, R.N. Anacine, a new benzodiazepine metabolite of *Penicillium aurantiogriseum* produced with other alkaloids in submerged fermentation. *J. Nat. Prod.* **1993**, *56*, 1707–1717. [[CrossRef](#)]
8. Wang, H.; Sim, M.M.J. Total solid phase syntheses of the quinazoline alkaloids: verrucines A and B and anacine. *Nat. Prod.* **2001**, *64*, 1497–1501. [[CrossRef](#)] [[PubMed](#)]
9. Grimblat, N.; Zanardi, M.; Sarotti, A.J. Beyond DP4: An improved probability for the stereochemical assignment of isomeric compounds using quantum chemical calculations of NMR shifts. *Org. Chem.* **2015**, *80*, 12526–12534. [[CrossRef](#)] [[PubMed](#)]
10. Huang, R.; Yi, X.X.; Zhou, Y.; Su, X.; Peng, Y.; Gao, C.H. An update on 2,5-diketopiperazines from marine organisms. *Mar. Drugs* **2014**, *12*, 6213–6235. [[CrossRef](#)] [[PubMed](#)]

11. Xu, W.F.; Mao, N.; Xue, X.J.; Qi, Y.X.; Wei, M.Y.; Wang, C.Y.; Shao, C.L. Structures and absolute configurations of diketopiperazine alkaloids chrysopiperazines A–C from the gorgonian-derived *Penicillium chrysogenum* Fungus. *Mar. Drugs* **2019**, *17*, 250. [[CrossRef](#)] [[PubMed](#)]
12. Cao, F.; Meng, Z.H.; Mu, X.; Yue, Y.F.; Zhu, H.J. Absolute configuration of bioactive azaphilones from the marine-derived fungus *Pleosporales* sp. CF09-1. *J. Nat. Prod.* **2019**, *82*, 386–392. [[CrossRef](#)] [[PubMed](#)]
13. Zhu, H.J. *Organic Stereochemistry-Experimental and Computational Methods*; KGaA; Wiley-VCH Verlag GmbH and Co.: Weinheim, Germany, 2015.
14. Cao, F.; Meng, Z.H.; Wang, P.; Luo, D.Q.; Zhu, H.J. Diplosporolones A and B, Dimeric azaphilones from a marine-derived *Pleosporales* sp. fungus. *J. Nat. Prod.* **2020**, *83*, 1283–1287. [[CrossRef](#)] [[PubMed](#)]
15. Bruhn, T.; Schaumlöffel, A.; Hemberger, Y.; Bringmann, G. SpecDis: Quantifying the comparison of calculated and experimental electronic circular dichroism spectra. *Chirality* **2013**, *25*, 243–249. [[CrossRef](#)] [[PubMed](#)]
16. Frisch, M.J.; Trucks, G.W.; Schlegel, H.B.; Scuseria, G.E.; Robb, M.A.; Cheeseman, J.R.; Scalmani, G.; Barone, V.; Mennucci, B.; Petersson, G.A.; et al. *Gaussian 09*; Gaussian Inc.: Wallingford, CT, USA, 2009.
17. Liao, L.J.; You, M.J.; Chung, B.K.; Oh, D.C.; Oh, K.B.; Shin, J.J. Alkaloidal metabolites from a marine-derived *Aspergillus* sp. fungus. *Nat. Prod.* **2015**, *78*, 349–354. [[CrossRef](#)] [[PubMed](#)]
18. Dong, L.; Shen, S.; Chen, W.; Lu, H.; Xu, D.; Jin, S.; Yang, Q.; Zhang, J. Glycosyl triazoles as novel insect β -N-acetylhexosaminidase OfHex1 inhibitors: Design, synthesis, molecular docking and MD simulations. *Bioorg. Med. Chem.* **2019**, *27*, 2315–2322. [[CrossRef](#)] [[PubMed](#)]
19. Liu, T.; Zhang, H.; Liu, F.; Chen, L.; Shen, X.; Yang, Q. Active-pocket size differentiating insectile from bacterial chitinolytic β -N-acetyl-D-hexosaminidases. *Biochem. J.* **2011**, *438*, 467–474. [[CrossRef](#)] [[PubMed](#)]
20. Liu, T.; Chen, L.; Zhou, Y.; Jiang, X.; Duan, Y.; Yang, Q.J. Structure, catalysis, and inhibition of OfChi-h, the lepidoptera-exclusive insect chitinase. *Biol. Chem.* **2017**, *292*, 2080–2088. [[CrossRef](#)] [[PubMed](#)]
21. Koska, J.; Spassov, V.Z.; Maynard, A.J.; Yan, L.; Austin, N.; Flook, P.K.; Venkatachalam, C.M. Fully automated molecular mechanics based induced fit protein-ligand docking method. *J. Chem. Inf. Model.* **2008**, *48*, 1965–1973. [[CrossRef](#)] [[PubMed](#)]
22. Scudiere, D.A.; Shoemaker, R.H.; Paull, K.D.; Monks, A.; Tierney, S.; Nofziger, T.H.; Currens, M.J.; Seniff, D.; Boyd, M.R. Evaluation of a soluble tetrazolium/formazan assay for cell growth and drug sensitivity in culture using human and other tumor cell lines. *Cancer Res.* **1988**, *48*, 4827–4833.



© 2020 by the authors. Licensee MDPI, Basel, Switzerland. This article is an open access article distributed under the terms and conditions of the Creative Commons Attribution (CC BY) license (<http://creativecommons.org/licenses/by/4.0/>).